[6] B. Djermakoye and J. A. Kong, "Radiative-transfer theory for the remote sensing of layered random media," *J. Appl. Phys.*, vol. 50, pp. 6600–6604, 1979.

[7] A. Mamouni, Y. Leroy, J. C. Vand De Velde, and L. Bellarbi, "Introduction to correlation microwave thermography," in *Proc. 12th European Microwave Conf.*, Helsinki, Finland, Sept. 1982.

[8] J. H. Jacobi, L. E. Larsen, "Microwave time delay spectroscopic imagery of isolated canine kidney," *Med. Phys.*, vol. 7, pp. 1–7, 1980.

[9] J. C. Bolomey, A. Izadneghadar, L. Jofre, C. Pichot, G. Peronnet, and M. Solaimani, "Microwave diffraction tomography for biomedical application," *IEEE Trans. Microwave Theory Tech.*, Nov. 1982.

[10] H. Ermert, F. Fülle, and D. Hiller, "Microwave computerized tomography," in *Proc. 11th European Microwave Conf.*, Amsterdam, The Netherlands, 1981, pp. 421–426.

[11] S. Rao, K. Santosh, and E. C. Cregg, "Computed tomography with microwaves," *Radiology*, vol. 135, pp. 769–780, 1980.

[12] A. R. Von Hippel, *Dielectrics and Their Applications*. New York: Wiley, 1964.

[13] D. S. Jones, *Theory of Electromagnetism*. New York: Pergamon, 1964, ch. 6, p. 335.

[14] C. Pichot, L. Jofre, G. Peronnet, A. Izadnegahdar, and J. C. Bolomey, "An angular spectrum method for inhomogeneous bodies reconstruction," in *Proc. IEEE-AP/S Symp.*, Albuquerque, NM, May 24–28, 1982, pp. 664–667.

[15] J. L. Guerquin-Kern, "Hyperthermie locale par microondes en thérapeutique cancérologique," *Thèse*, Strasbourg, 20 Jun. 1980.

[16] S. Al Adhami, A. P. Anderson, and J. C. Bennet, "A novel radar array and its imaging properties," *IEEE Trans. Antennas Propagat.*, vol AP-27, no. 4, pp 567–570, 1979.

[17] M. Melek and A. P. Anderson, "Theoretical studies of localised tumour using focused microwave arrays," *IEE Proc.*, vol. 127, pt F, no. 4, Aug. 1980, pp. 319–321.

[18] J. Robert, C. Marchal, J. M. Escanye, P. Thouvenot, M. L. Gaulard, and A. Tosser, "Utilisation de la vélocimétrie ultrasonore pour le contrôle de l'hyperthermie," in *Proc. Int. Symp. Biomédical Thermology*, Strasbourg, Jul. 1981, p. E-73.

[19] R. Maini, M. F. Iskander, C. H. Durney, and M. Berggren, "On the sensitivity and the resolution of microwave imaging using ART," *Proc. IEEE*, vol. 69, no. 11, Nov. 1981, pp. 1517–1519.

[20] B. G. Fallone, P. R. Moran, and E. B. Podgorsak, "Non invasive thermometry with a clinical X-ray CT scanner," *Med. Phys.*, vol. 9, no. 5, pp. 715–721, Sept.–Oct. 1982.

On the Transient Analysis of Circuits Containing Multiple Diodes

P. A. BLAKEY AND R. K. FROELICH

Abstract —**Multiple-diode circuits are increasingly being used for power combining at microwave frequencies. This paper presents a method for the transient analysis of such circuits. The method exploits the cold-capacitance–particle-current decomposition of semiconductor diodes and is simpler, more efficient, and more accurate than previously proposed approaches to the problem.**

I. Introduction

Hiraoka [1] recently considered the problem of transient analysis of multiple nonequivalent transit-time diodes embedded in a circuit. This is a problem of considerable practical importance, especially in the area of power combining. The method demonstrated by Hiraoka combines the finite-difference equations associated with time-domain device simulation, together with the circuit equations, into a single matrix equation for the whole system. The implementation is inherently implicit and requires the inversion of a large matrix at each time step. The coefficients of the matrix to be inverted are time dependent and must be evaluated at each time step. Repeated inversion of a large matrix makes the method extremely expensive. The cost also increases much faster than linearly with the number of devices considered.

The purpose of this note is to present an alternative procedure which is simpler, more efficient, at least as accurate, and for which the cost increases only linearly with the number of devices considered.

Manuscript received January 26, 1983; revised May 2, 1983. This work was supported by Air Force Avionics Laboratory, Wright-Patterson Air Force Base, OH.

P. A. Blakey is with the Electron Physics Laboratory, Department of Electrical and Computer Engineering, University of Michigan, Ann Arbor, MI 48109.

R. K. Froelich is with Watkins Johnson Co., Palo Alto, CA.

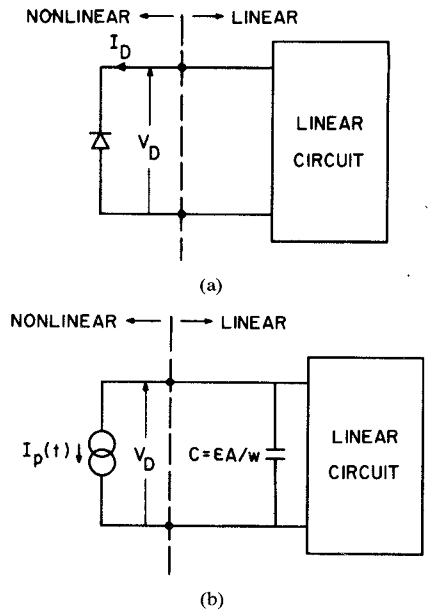

Fig 1. The diode-circuit partitioning. (a) Before the capacitance–particle-current decomposition. (b) After the capacitance–particle-current decomposition. $\{I_p(t) = (1/w)\int_0^w [I_e(x,t)+I_h(x,t)]\,dx\}$.

II. Alternative Methods

Most previous work has partitioned the system into a linear (circuit) part and a nonlinear (diode) part as in Fig. 1(a). The circuit part is treated using the well-established methods of linear system theory, and the diode part is treated using time-domain simulation. The time-domain simulation can be implicit or explicit. Different methods of linear system theory lead to different implementations. Evans and Scharfetter [2] used an impulse response/convolution integral approach with the convolution implemented using an FFT. Brazil and Scanlan [3] used state-space methods. Efficient procedures for handling mixed lumped-distributed circuits were developed by Mains *et al.* [4]. Care must be taken with the interfacing. An iterative procedure, involving at least two diode solutions, is generally adopted to obtain reasonable self-consistency between diode and circuit current and voltage. Avoidance of this iteration is a major motivation of Hiraoka's approach.

Blakey *et al.* [5] used the same device–circuit partitioning with an explicit diode/circuit interaction. This method is efficient but not very general; the circuit element next to the diode has to be an inductance, and for small enough values of inductance the accuracy of the method can be unacceptably low.

III. An Accurate and Efficient Explicit Method

The authors' present method involves a modification of the diode/circuit partitioning. The cold-capacitance–particle-current generator decomposition (see Appendix I) is performed for the diode, and the cold capacitance is transferred to the linear side of the partition, as in Fig. 1(b). Device and circuit time stepping then reduces to the following explicit procedure.

a) Calculate "new" carrier concentrations using the "old" electric field.

b) Calculate the new diode voltage as the response of the linear system to the particle-current driving function.

c) Calculate the new electric field by solving Poisson's equation for the new voltage and carrier concentrations.

The particle current driving function in step b may be calculated using the "old" carrier concentrations or an average of "old" and "new" values. For simple loads step b can often be implemented as an explicit function of the diode particle current and "old" circuit values (see Appendix II for an example). For more complicated loads it is easier to use state-space methods and the Mains *et al.* techniques, both of which are well suited for efficient numerical implementation.

The extension of this method to multiple nonequivalent devices is trivial. Each device is split into a cold capacitance, which is included in the linear circuit, and a particle-current driving function. The circuit now has multiple inputs but these are routinely handled by the methods of linear system theory.

This implementation of multiple diode–circuit simulation has proved completely satisfactory; it yields an implementation which is simple, accurate, and efficient. It is being used to model current sharing, degradation characteristics, and instability phenomena in IMPATT power combining circuits, has been used to demonstrate push–pull TRAPATT circuit operation, and is generally applicable to other multidiode circuits. This work will be the subject of a future paper.

IV. Discussion

It is instructive to consider sources of error in the present scheme and in Hiraoka's scheme. These sources can be divided into errors introduced in the device simulation and errors introduced in the device–circuit implementation.

Hiraoka's underlying device simulation is basically first-order explicit in time; the implicit nature of the device–circuit interaction does not mean that the device simulation is second-order accurate. Significant sources of error in this first-order implementation, and some explicit corrections to improve the accuracy, were discussed elsewhere [5]. Hiraoka's device–circuit implementation appears to be second-order accurate, once it is assumed that the device currents are as predicted by the simulation.

The authors' philosophy of device simulation [5], [6] is to implement quasi-second-order schemes using the following: explicit schemes with correction terms, predictor–corrector algorithms, and recurrence solution (Potter [7]) of tridiagonal matrix equations. Implicit schemes which require full matrix inversion are currently avoided because their expense still severely limits their usefulness. The device–circuit implementation outlined in Section III can be exact once it is assumed that the device particle currents have the form predicted by the quasi-second-order device simulation. Most numerical error in the overall scheme is thus in the extent to which the changes in particle current within a time step are not taken into account. Changes due to generation and recombination are taken into account to first-order if the "average" procedure is used for step b of the algorithm. In this case, the main remaining source of error is associated with changes in carrier velocity caused by field changes within the time step. However, these changes impose a limit on the time step that can be used in the device simulation [5]. This ensures that in practice the error associated with the device–circuit implementation is always acceptably small.

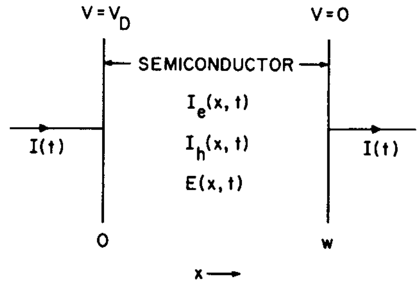

Fig. 2. Geometry and notation for the cold capacitance–particle-current generator decomposition.

Overall, the method described here will generally be more accurate, as well as more efficient, than Hiraoka's method.

Appendix I
The Capacitance–Particle-Current Decomposition

In terms of the geometry and notation indicated in Fig. 2, the differential form of the statement of current continuity in one spatial dimension can be written as

$$I(t)=I_e(x,t)+I_h(x,t)+\epsilon A\frac{\partial E(x,t)}{\partial t} \tag{A1}$$

where I is the total current, I_e is the current carried by electrons, I_h is the current carried by holes, ϵ is the dielectric constant, A is the cross-sectional area of the diode, and E is the electric field. (Equation (A-1) is trivially derived from the Maxwell equation $\nabla\times\boldsymbol{H}=\boldsymbol{J}_{\text{cond}}+(\partial\boldsymbol{D}/\partial t)$ and the vector identity $\nabla.(\nabla\times\boldsymbol{H})=0$.)

Integrating (A1) from 0 to w and dividing by w leads to the integral form of the statement of current continuity

$$I(t)=\frac{1}{w}\int_0^w[I_e(x,t)+I_h(x,t)]\,dx+\frac{\epsilon A}{w}\frac{\partial V_D}{\partial t}. \tag{A2}$$

Equation (A2) shows that the total current is that of the displacement current flowing through the geometric or "cold" capacitance $C=\epsilon A/w$, in parallel with a "particle" current I_p, which is the spatially averaged value of the sum of the electron and hole currents. Equation (A2) is quite general, once it is assumed that there are no spatial variations in the y- or z-directions. In practice, (A2) is usually applied only to the active region of the device; substrate and contact regions are conveniently represented by equivalent series resistances.

Appendix II
DC Current and RF Voltage Control

Transit-time device studies generally seek to characterize device admittance as a function of RF voltage for user-specified dc currents and frequencies. This can be done using the circuit shown in Fig. 3. From Kirchhoff's equations

$$I_{\text{dc}}=I_p(t)+C_D\frac{dV_D(t)}{dt}+I_L(t)$$

$$V_D(t)=V_c(t)+V_{\text{RF}}(t)$$

and

$$\frac{dV_c(t)}{dt}=\frac{I_L(t)}{C_B}.$$

These equations can be solved for $V_D(t)$, yielding

$$V_D(t_0+\Delta t)=V_D(t_0)+(C_B+C_D)^{-1}$$
$$\cdot\left(I_{\text{dc}}\Delta t-\int_{t_0}^{t_0+\Delta t}I_p(t)\,dt+C_B\int_{t_0}^{t_0+\Delta t}\frac{dV_{\text{RF}}(t)}{dt}dt\right).$$

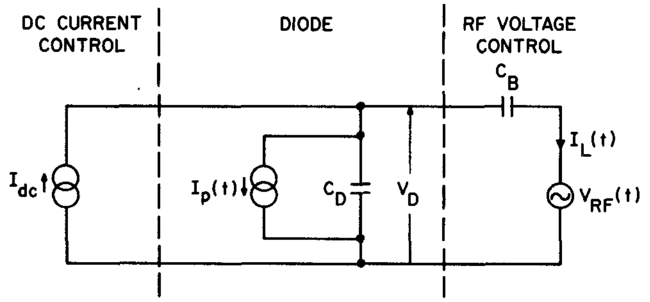

Fig. 3. Load configuration for dc current and RF voltage control.

If $V_{\mathrm{RF}}(t) = V_{\mathrm{RF}} \sin \omega t$ and $I_p(t)$ is assumed to vary linearly between $I_p(t_0)$ and $I_p(t_0 + \Delta t)$, then

$$V_D(t_0 + \Delta t) = V_D(t_0) + (C_B + C_D)^{-1} \cdot \Big(I_{\mathrm{dc}} \Delta t + \frac{\Delta t}{2}\left[I_p(t_0 + \Delta t) + I_p(t_0) \right] + C_B V_{\mathrm{RF}} \left[\sin \omega (t_0 + \Delta t) - \sin \omega t_0 \right] \Big).$$

The value of C_B is chosen to avoid parametric and bias instabilities [3].

ACKNOWLEDGMENT

It is a pleasure to acknowledge useful discussions with Mr. J. East, Dr. R. K. Mains, and Professors G. I. Haddad and D. F. Peterson.

REFERENCES

[1] K. Hiraoka, "Transient analysis of two semiconductor devices under circuit-loaded conditions," *IEEE Trans. Electron Devices*, vol. ED-29, pp. 1617–1621, Oct. 1982.
[2] W. J. Evans and D. L. Scharfetter, "Characterization of avalanche diode TRAPATT oscillators," *IEEE Trans. Electron Devices*, vol. ED-17, pp. 397–404, May 1970.
[3] T. J. Brazil and S. O. Scanlan, "Self-consistent solutions for IMPATT diode networks," *IEEE Trans. Microwave Theory Tech.*, vol. MTT-29, pp. 26–31, Jan. 1981.
[4] R. K. Mains, N. A. Masnari, and G. I. Haddad, "Theoretical investigations of TRAPATT amplifier operation," *IEEE Trans. Microwave Theory Tech.*, vol. MTT-28, pp. 1070–1076, Oct. 1980.
[5] P. A. Blakey, R. A. Giblin, and A. J. Seeds, "Large-signal, time-domain modeling of avalanche diodes," *IEEE Trans. Electron Devices*, vol. ED-26, pp. 1718–1728, Nov. 1979.
[6] R. K. Froelich, "Computer modeling of millimeter-wave IMPATT diodes," Ph.D. dissertation, The University of Michigan, Ann Arbor, MI, May 1982.
[7] D. Potter, *Computational Physics*. New York: Wiley-Interscience, pp. 88–91, 1973.

Letters

Comment on "Heat Transfer in Surface-Cooled Objects Subject to Microwave Heating"

T. C. GUO, SENIOR MEMBER, IEEE, W. W. GUO, SENIOR MEMBER, IEEE, L. E. LARSEN, SENIOR MEMBER, IEEE, AND J. H. JACOBI, SENIOR MEMBER, IEEE

In the above paper[1], Foster *et al.* derived the following equation for the temperature T^* at the center of a spherical tissue:

$$T^* - T_0 = \frac{Qa^2}{6k}\left(1 + \frac{2}{\mathrm{Bi}(U_\infty)}\right) \tag{1}$$

where T_0 is ambient temperature of the cooling fluid, Q the volumetric heat generation by the microwave irradiation, a the radius of the sphere, k the thermal conductivity of the tissue, U_∞ the free-stream velocity of the cooling fluid, and Bi the Biot number. The value of $2/\mathrm{Bi}$ depends on the coolant-flow velocity, vanishing for rapid coolant flow and approaching $2k/k_f$ for a stagnant coolant, with k_f being the thermal conductivity of the coolant.

While the above formulation agrees with our recent conclusions [2], Foster *et al.* have exaggerated the expected temperature rise for ocular lens by statements in the abstract and the concluding remarks. Take $k = 0.7k_f$ and $Q = 100$ mW/cm^3, as the authors suggested, and $k_f = 6.23$ mW/cm $-$ °C, then the temperature rise at the center of a spherical tissue with 0.15-cm radius is between 0.086°C and 0.21°C, where the upper limit applies to a spherical tissue in a stagnant coolant. With respect to thermally mediated pathogenicity, this range of temperature increase is negligible; but the authors stated in the abstract that there would be significant temperature rise without providing a specific value or justification.

Foster *et al* are frankly mistaken in their calculation of the temperature gradient in the ocular studies of Stewart-DeHaan *et al.* The authors stated that "the maximum temperature increase is 0.6°C to 6°C for SAR's of 120 mW/g to 1200 mW/g." This value is erroneous since it is based upon a lens diameter of 0.7 cm. Such a value is more suitable for bovine than murine subjects. Since the gradient is a function of the radius squared, a difference between an assumed radius of 0.35 cm as opposed to an actual radius of 0.15-cm accounts for the difference between our result of ca. 1°C and their result of ca. 6°C at the highest SAR. Obviously, the gradient scales linearly with SAR such that at the lowest SAR the gradient is comparable to the noise in the thermoregulator.

Manuscript received December 20, 1982.
T. C. Guo and W. W. Guo are with the Johns Hopkins University Applied Physics Laboratory, Laurel, MD 20707.
L. E. Larsen and J. H. Jacobi are with the Walter Reed Army Institute of Research, Washington, D.C.
[1] Foster *et al.*, *IEEE Trans. Microwave Theory Tech.*, vol. MTT-30, pp. 1158–1166, Aug. 1982.

0018-9480/83/0900-0783$01.00 ©1983 IEEE